The walk-sum method for simulating quantum many-body systems

P-L Giscard[1], M Kiffner[2,1] and D Jaksch[1,2]

[1]Clarendon Laboratory, Department of Physics, University of Oxford, Parks Road, Oxford OX1 3PU, United Kingdom
[2]Centre for Quantum Technologies, National University of Singapore, 3 Science Drive 2, Singapore 117543

E-mail: p.giscard1@physics.ox.ac.uk

Abstract. We present the method of walk-sum to study the real-time dynamics of interacting quantum many-body systems. The walk-sum method generates explicit expressions for any desired pieces of an evolution operator U independently of any others. The computational cost for evaluating any such piece at a fixed order grows polynomially with the number of particles. Walk-sum is valid for systems presenting long-range interactions and in any geometry. We illustrate the method by means of two physical systems.

PACS numbers: 02.70.-c, 02.10.Yn, 02.10.Ox, 32.80.Rm

Submitted to: *J. Phys. A: Math. Theor.*

1. Introduction

The quality of control over atomic systems in state of the art experiments is such that one can now address and observe quantum evolutions of individual atoms in optical-lattices [1, 2, 3, 4]. Additionally, coherent inter-atomic and light-matter interactions can be made strong enough to occur on short time-scales compared to incoherent processes. This reveals the system's unitary evolution at the individual constituent level which is of fundamental interest in the study of quantum many-body phenomena. Several applications like quantum simulation and quantum computing schemes also rely on this information [5]. On the other hand, the theoretical simulation of such non-equilibrium many-body dynamics is very challenging, mainly due to the exponentially large number of relevant degrees of freedom.

This has led to the rise of an active area of research focused on the development of theoretical methods to simulate the dynamics of quantum systems. Among the most well known techniques are the Density Matrix Renormalization Group method [6], related Tensor Network approaches [7] and the Time-Evolving Block Decimation method [8]. These techniques have proven to be very successful in their respective domains of applicability (e.g. [9, 10, 11]), i.e. mostly 1D systems with nearest neighbour interactions. On the contrary, and in spite of extensive work in the field, very few techniques exist in 2D and 3D [12, 13] and for systems exhibiting long-range interactions.

In this article we introduce an approach to the real-time evolution of quantum systems that is not restricted by the system geometry and works in the presence of long-range interactions. Our method, termed walk-sum, describes quantum evolutions as resulting from a superposition of all the histories of the system, a discrete analog to Feynman path-integrals. We show that with walk-sum one can evaluate arbitrarily chosen pieces of the full evolution operator U independently of one another. Additionally, we show that each piece can be approximated efficiently, i.e. in a number of operations that scales polynomially in the number N of involved particles.

This article is organised as follows. In section 2 we introduce the walk-sum approach for the simulation of quantum many-body systems. In order to illustrate the method and its capabilities, we discuss two physical examples in section 3. The computational cost for implementing the walk-sum method is described in section 4. Finally, we present a conclusion and outlook in section 5.

2. The walk-sum method

We consider a quantum many-body system $\mathbb{S}$ to be comprised of two parts S and S'. The method of walk-sum is based on the following observation: If S' is a large set of constituents whose dynamics is frozen, then all interactions between S and S' can be evaluated exactly and the evolution of S is described by a small effective Hamiltonian. Walk-sum expresses the true many-body dynamics in terms of such simple situations with a frozen S' and a few evolving constituents S. This approach might seem similar in essence to mean field theory where an atom of interest interacts with a field resulting from the mean behaviour of all other particles. The difference is that here we make the mapping from many-body to few-body dynamics exact, that is we make S interact with all possible fields it could be subjected to depending on the configuration of S'.

In practice, the walk-sum method divides the matrix representing the time evolution operator of a finite-dimensional quantum system into small pieces. These pieces are called conditional evolution operators and are introduced in section 2.1, where we describe the general approach of the method. In section 2.2 we derive an equation that allows one to calculate any conditional evolution operator and therefore any desired piece of the full evolution operator. We then show in section 2.3 that the generation of conditional evolution operators can be represented by walks on a graph. This facilitates the evaluation of the walk-sum expression. In section 2.4 we address the evaluation of conditional evolution operators via Laplace transforms. Finally, we demonstrate how the method allows one to evaluate expectation values and conditional expectation values in section 2.5.

2.1. Model system and general approach

We consider a quantum many-body system $\mathbb{S}$ that is described by a time-independent Hamiltonian H and comprised of N physical constituents. The state space of the kth constituent is spanned by d_k internal levels, where d_k can be different for every k. Let $\{|i_k\rangle\}$ be an orthonormal basis of length d_k associated with constituent k, and $P_{k,i} = |i_k\rangle\langle i_k|$ is the projector onto state $|i_k\rangle$. Next we split the system $\mathbb{S}$ into two parts S and S'. Here S is taken to be constituent s, and all remaining constituents are grouped in S'. Note that constituent s can be comprised of one or several physical

particles. We define so-called projector-lattices

$$\hat{\varepsilon}_\mu = \otimes_{k\in S'} P_{k,i_k} \otimes \mathcal{I}_s = \overbrace{|\mu\rangle\langle\mu|}^{\text{Acts on } S'} \otimes \overbrace{\mathcal{I}_s}^{\text{Acts on } S} \tag{1}$$

that are projection operators in the state space of the full system $\mathbb{S}$. The index μ is a short-hand notation for the configuration onto which S' is projected and $\mathcal{I}_s$ is the identity operator on S. There is a total of $\prod_{k\neq s}^{N} d_k$ different projector-lattices corresponding to all possible combinations of projectors P_{k,i_k}. Projector-lattices are themselves orthogonal projectors and the ensemble of all possible projector-lattices is closed,

$$\hat{\varepsilon}_\nu \hat{\varepsilon}_\mu = \delta_{\nu,\mu}\, \hat{\varepsilon}_\nu, \quad \sum_\nu \hat{\varepsilon}_\nu = \mathcal{I}, \tag{2}$$

where $\mathcal{I}$ is the identity operator on the state-space of the whole many-body system $\mathbb{S}$. We emphasise that our method will work for any set of projector lattices $\{\hat{\varepsilon}_\nu\}$ that fulfil Eq. (2).

Next we partition the time evolution operator $U = \exp[-iHt]$ (throughout this article we set $\hbar = 1$) into submatrices with projector lattices,

$$\hat{\varepsilon}_\nu U(t) \hat{\varepsilon}_\mu = \otimes_{k\in S'} T_{k,i_k\leftarrow j_k} \otimes U_{\nu\leftarrow\mu}(t) = \underbrace{|\nu\rangle\langle\mu|}_{\text{Acts on } S'} \otimes \underbrace{U_{\nu\leftarrow\mu}(t)}_{\text{Acts on } S}. \tag{3}$$

Here $T_{k,i\leftarrow j} = |i_k\rangle\langle j_k|$ denotes a transition operator in subsystem k, and $U_{\nu\leftarrow\mu}(t)$ is a so-called conditional evolution operator that is represented by a (small) $d_s \times d_s$ matrix. $U_{\nu\leftarrow\mu}(t)$ generates the time evolution of subsystem S provided that (i) the remaining many-body system S' was initially in configuration $|\mu\rangle$, and (ii) the state of S' at time t is given by $|\nu\rangle$. The closure relation in Eq. (2) implies that the full time evolution operator $U(t)$ can be represented in terms of conditional evolution operators,

$$U(t) = \sum_{\nu,\,\mu} \Big\{ \underbrace{|\nu\rangle\langle\mu|}_{\text{Acts on } S'} \otimes \underbrace{U_{\nu\leftarrow\mu}(t)}_{\text{Acts on } S} \Big\}. \tag{4}$$

The method of walk-sum allows one to compute conditional evolution operators efficiently, i.e. in a number of operations scaling polynomially in the number of involved particles, and independently of one another. If in a particular physical problem only a small subset of all possible configurations of S' is relevant, then our approach allows one to approximate the full time evolution with a moderate computational effort [14].

2.2. Derivation of the conditional evolution operators

In this section we derive an explicit expression for conditional evolution operators that allows one to generate them without calculating the full time evolution operator. To this end, we write the time evolution operator $U(t)$ of the complete system $\mathbb{S}$ as

$$U(t) = \exp[-iHt] = \lim_{\delta t\to 0} \prod_{n=1}^{M} \delta U = \lim_{\delta t\to 0} \prod_{n=1}^{M} \Big\{ \sum_\alpha \hat{\varepsilon}_\alpha\, \delta U \Big\}, \tag{5}$$

where $\delta U = \mathcal{I} - iH\delta t$ is the infinitesimal evolution operator from $(n-1)\delta t$ to $n\delta t$ and $M = t/\delta t$. In the last step in Eq. (5) we inserted the closure relation for projector

lattices [see Eq. (2)]. In the following, we derive explicit expressions for the conditional time evolution operators $U_{\nu\leftarrow\mu}(t)$ by a re-summation of terms arising in $\hat{\varepsilon}_\nu U(t)\hat{\varepsilon}_\mu$. Let us first focus on $\hat{\varepsilon}_\nu U(t)\hat{\varepsilon}_\nu$, and in particular the term where all intermediate projector lattices $\hat{\varepsilon}_\alpha$ in Eq. (5) are all equal to $\hat{\varepsilon}_\nu$,

$$\mathcal{U}_\nu^{(0)} = \hat{\varepsilon}_\nu \prod_{n=1}^{M} \{\hat{\varepsilon}_\nu\, \delta U\}\hat{\varepsilon}_\nu = \hat{\varepsilon}_\nu \delta U \hat{\varepsilon}_\nu \delta U \ldots \hat{\varepsilon}_\nu \delta U \hat{\varepsilon}_\nu. \tag{6}$$

The physical meaning of this term is the following. First S' is projected into configuration ν, then δU evolves the full system $\mathbb{S}$ from 0 to δt. Then $\hat{\varepsilon}_\nu$ projects S' onto configuration ν, followed by a time evolution of $\mathbb{S}$ for δt, and so on. In the limit $\delta t \to 0$, S' is frozen by continuous (Zeno) measurements of $|\nu\rangle\langle\nu|$ and S evolves freely under the influence S' in configuration ν. We find

$$\lim_{\delta t\to 0} \mathcal{U}_\nu^{(0)} = \lim_{\delta t\to 0} \prod_{n=1}^{M} (\hat{\varepsilon}_\nu - i\,\hat{\varepsilon}_\nu H \hat{\varepsilon}_\nu \delta t) = u_\nu(t,0), \tag{7}$$

where

$$u_\nu(t,t') = \hat{\varepsilon}_\nu\, e^{-i\,\hat{\varepsilon}_\nu H \hat{\varepsilon}_\nu (t-t')} \tag{8}$$

is a so-called Zeno evolution operator that evolves S between times t and t' while S' is frozen in configuration $|\nu\rangle$. Zeno-evolution operators obey the following relations

$$u_\nu u_\mu = 0 \quad \text{if } \nu \neq \mu, \quad \hat{\varepsilon}_\nu u_\nu = u_\nu \hat{\varepsilon}_\nu = u_\nu, \quad \text{and} \quad u_\nu^\dagger u_\nu = u_\nu u_\nu^\dagger = \hat{\varepsilon}_\nu. \tag{9}$$

Next we discuss the projection $\hat{\varepsilon}_\nu U(t)\hat{\varepsilon}_\mu$ for $\mu \neq \nu$ and focus on those terms that are of the form

$$\mathcal{U}_{\nu\mu}^{(1)} = \quad \hat{\varepsilon}_\nu \delta U \hat{\varepsilon}_\nu \delta U \ldots \hat{\varepsilon}_\nu \delta U \hat{\varepsilon}_\nu \quad \delta U \quad \hat{\varepsilon}_\mu \delta U \hat{\varepsilon}_\mu \delta U \ldots \hat{\varepsilon}_\mu \delta U \hat{\varepsilon}_\mu \tag{10a}$$

$$= -i\delta t \underbrace{\hat{\varepsilon}_\nu \delta U \hat{\varepsilon}_\nu \delta U \ldots \hat{\varepsilon}_\nu \delta U \hat{\varepsilon}_\nu}_{=\mathcal{X}\ (M-M'\ \text{times}\ \delta U)} \hat{\varepsilon}_\nu H \hat{\varepsilon}_\mu \underbrace{\hat{\varepsilon}_\mu \delta U \hat{\varepsilon}_\mu \delta U \ldots \hat{\varepsilon}_\mu \delta U \hat{\varepsilon}_\mu}_{=\mathcal{Y}\ (M'-1\ \text{times}\ \delta U)}, \tag{10b}$$

where we employed $\hat{\varepsilon}_\nu \delta U \hat{\varepsilon}_\mu = -i\delta t\, \hat{\varepsilon}_\nu H \hat{\varepsilon}_\mu$. Now let $t = M\delta t$ and $t' = M'\delta t$. The term $\mathcal{U}_{\nu\mu}^{(1)}$ can be interpreted as follows. Initially S' is projected into state $|\mu\rangle$ and we observe that $\lim_{\delta t\to 0} \mathcal{Y} = u_\mu(t',0)$. This is the Zeno evolution operator for S that keeps S' static in state $|\mu\rangle$ between 0 and t'. Then the subsystem S' makes a jump from configuration $|\mu\rangle$ to configuration $|\nu\rangle$ [term $\hat{\varepsilon}_\nu H \hat{\varepsilon}_\mu$], followed by the evolution of S between t' and t with S' frozen in state $|\nu\rangle$ [term $\mathcal{X}$ in Eq. (10a) fulfils $\lim_{\delta t\to 0} \mathcal{X} = u_\mu(t,t')$]. Note that the limit $t \to 0$ cannot be taken directly in $\mathcal{U}_{\nu\mu}^{(1)}$, since there are $M \to \infty$ ($\delta t \to 0$) similar terms appearing in $\hat{\varepsilon}_\nu U(t)\hat{\varepsilon}_\mu$ that differ from $\mathcal{U}_{\nu\mu}^{(1)}$ only in the position of the jump operator $\hat{\varepsilon}_\nu H \hat{\varepsilon}_\mu$, i.e. the time t' at which S' makes the transition $\mu \to \nu$. Summing over all these terms and taking the limit $t \to 0$ yields

$$\lim_{\delta t\to 0} \sum_{q=1}^{M} -i\delta t\, \mathcal{X}(t, q\delta t)\, H\, \mathcal{Y}(q\delta t - \delta t, 0) = -i \int_0^t u_\nu(t,t') H u_\mu(t',0) dt', \tag{11}$$

and the integral is thus a continuous sum over the time for the jump $\mu \to \nu$ to occur. The full expansion of $\hat{\varepsilon}_\nu U(t)\hat{\varepsilon}_\mu$ also contains terms with an arbitrary number

of intermediary configurations η_q between the initial and final configurations μ and ν, respectively. For each of these configurations, the jump $\eta_q \to \eta_{q+1}$ can occur at any time t_q between 0 and the next jump at time t_{q+1}. Thus

$$\hat{\varepsilon}_\nu U(t)\hat{\varepsilon}_\mu = u_\nu(t,0)\delta_{\mu,\nu} + \tag{12}$$
$$\sum_{n=1}^{\infty} i^{-n} \sum_{\eta_1,\ldots,\eta_n} \int_0^t \int_0^{t_n} \ldots \int_0^{t_2} u_\nu(t,t_n) H u_{\eta_n}(t_n,t_{n-1}) H \ldots u_{\eta_1}(t_2,t_1) H u_\mu(t_1,0) dt_1 \ldots dt_n,$$

where the sum over n counts the number of jumps between different intermediate configurations η_q. The result in Eq. (12) can also be formally derived with graph theoretical methods [15]. In addition, we provide a short alternative proof of this result in Appendix A, demonstrating that Eq. (12) can also be regarded as a perturbative expansion of the time evolution operator in the transitions underwent by S'. While S evolves smoothly in time, Eq. (12) describes S' as evolving stroboscopically in its state-space: e.g. S' is static in configuration μ from 0 to time t_1, then jumps instantaneously to another configuration ν where its stays static until t_2, and so on. Each succession of configurations adopted by S' from 0 to time t is a possible history of S'. The dynamics of S as obtained by Eq. (12) then appears as the superposition of the effects on S of all the possible histories of S'.

The expression for $\hat{\varepsilon}_\nu U(t)\hat{\varepsilon}_\mu$ in Eq. (12) simplifies greatly on using the mixed-product property of the tensor product $(A \otimes B)(C \otimes D) = AC \otimes BD$. Indeed, this implies that for any two projector-lattices $\hat{\varepsilon}_\nu$ and $\hat{\varepsilon}_\mu$ there exist small $d_s \times d_s$ matrices H_ν, $H_{\nu\leftarrow\mu}$ and $U_{\nu\leftarrow\mu}(t)$ such that

$$\hat{\varepsilon}_\nu H \hat{\varepsilon}_\nu = \otimes_{k\in S'} P_{k,i_k} \otimes H_\nu = \overbrace{|\nu\rangle\langle\nu|}^{\text{Acts on } S'} \otimes \overbrace{H_\nu}^{\text{Acts on } S}, \tag{13a}$$
$$u_\nu(t) = \otimes_{k\in S'} P_{k,i_k} \otimes e^{-iH_\nu t} = |\nu\rangle\langle\nu| \otimes e^{-iH_\nu t}, \tag{13b}$$
$$\hat{\varepsilon}_\nu H \hat{\varepsilon}_\mu = \otimes_{k\in S'} T_{k,i_k\leftarrow j_k} \otimes H_{\nu\leftarrow\mu} = |\nu\rangle\langle\mu| \otimes H_{\nu\leftarrow\mu}. \tag{13c}$$

The H_ν matrices are called statics because they physically correspond to small effective Hamiltonians driving S when S' is static in $|\nu\rangle$, i.e. frozen in configuration ν. Similarly, the $H_{\nu\leftarrow\mu}$ matrices are called flips and represent how a jump of S' from μ to ν affects the dynamics of S. The H_ν are Hermitian and $(H_{\nu\leftarrow\mu})^\dagger = H_{\mu\leftarrow\nu}$. Using these matrices and the mixed-product property we can completely separate the evolution of S from the evolution of S'. It follows that Eq. (12) is equivalent to

$$U_{\nu\leftarrow\mu}(t) = e^{-iH_\nu t}\delta_{\mu,\nu} + \sum_{n=1}^{\infty} i^{-n} \tag{14}$$
$$\times \sum_{\eta_1,\ldots,\eta_n} \int_0^t \int_0^{t_n} \ldots \int_0^{t_2} e^{-iH_\nu(t-t_n)} H_{\nu\leftarrow\eta_n} e^{-iH_{\eta_n}(t_n-t_{n-1})} H_{\eta_n\leftarrow\eta_{n-1}} \ldots e^{-iH_\mu t_1} dt_1 \ldots dt_n.$$

Note that this expression for $U_{\nu\leftarrow\mu}(t)$ only comprises $d_s \times d_s$ matrices. With Eq. (14) we achieved to transform the complications associated with the real-time dynamics of a quantum many-body system into the sum over the intermediary configurations $\eta_1, \ldots \eta_n$ of S'. In the following section 2.3, we show that each contribution to the sum in Eq. (14) can be represented as a walk on a graph. This visualisation clearly brings out all the physical processes contributing to $U_{\nu\leftarrow\mu}$. Most importantly, we show that this graphical representation facilitates the evaluation of Eq. (14) substantially.

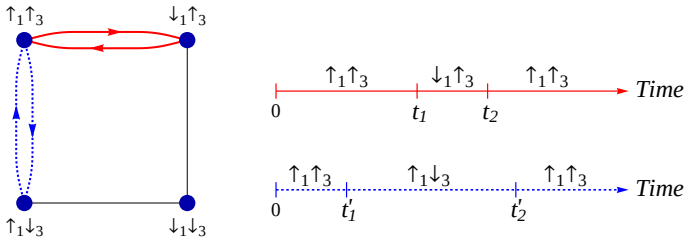

(a) (b)

Figure 1: (Colour Online). (a) A square, the graph $\mathcal{G}$ of all configurations available to S', here an ensemble of two spin-1/2 particles labelled 1 and 3. Each edge represents a transition allowed by the Hamiltonian in Eq. (15). Highlighted in solid-red and dashed-blue are two walks of S' on $\mathcal{G}$, i.e. two possible histories of S' between time 0 and time t. (b) The histories of S' represented by the solid-red and dashed-blue walks in (a) where t_1, t_2, t'_1 and t'_2 are the jumping times. This representation of the histories can also be thought of as the discrete equivalent of Feynman diagrams, the physical processes being the spin flips caused by the Hamiltonian.

2.3. Representing the time evolution on a graph

The sum over the intermediary configurations η_q in Eq. (14) can be interpreted as a sum over the histories of S', a history being a succession of configurations adopted by S' from 0 to time t. To visualise the histories, we construct a graph $\mathcal{G}$ as follows:
i) For each configuration ν available to S', draw a vertex v_ν.
ii) For each non-zero flip, i.e. when S' is allowed to make a transition between two specific configurations μ and ν, draw an edge between v_μ and v_ν.
Now we can see that a multiplication by $e^{-iH_\nu \tau}$ in Eq. (14) represents the evolution of S while S' is stationary at vertex v_ν during time τ. A multiplication by $H_{\nu\leftarrow\mu}$ in Eq. (14) corresponds to an instantaneous move of S' along the edge $v_\mu \to v_\nu$. Consequently, the histories of S' appear as walks on $\mathcal{G}$ and their superposition is obtained as the sum over all the walks, in complete analogy with Feynman path-integrals. If the system had continuous degrees of freedom, the sum over histories, that is the sum over the walks, would become an integral over histories which corresponds to an integral over the walks, i.e. a Feynman path-integral. An equivalent to the Feynman diagrams also exists in our situation: this is the succession of physical processes underwent by S' during a history. Finally, from a practical point of view, the graph itself facilitates the visualisation of the histories of S' contributing to a given conditional evolution operator. To clarify these notions, we now construct the graph of a small physical system.

Example. Consider a 1D chain of three spin-1/2 particles, and choose S to be the central spin, labelled 2. S' is thus comprised of the other two spins 1 and 3. Suppose that the Hamiltonian of the system is

$$H = \sum_{i=1}^{3} \Delta\, \sigma_x^i + \sum_{i=1}^{2} J\, \sigma_z^i \sigma_z^{i+1}, \tag{15}$$

where $\sigma_{x,z}$ are Pauli matrices and Δ and J are two real parameters. There are $2^2 = 4$ orthogonal configurations available to S' and $\mathcal{G}$ has 4 vertices. Indeed, choosing the

configurations to be those specifying the direction of the spins along the z-axis‡, the operator lattices are $\hat{\varepsilon}_{\uparrow_1\uparrow_3} = |\uparrow_1\uparrow_3\rangle\langle\uparrow_1\uparrow_3|$, $\hat{\varepsilon}_{\uparrow_1\downarrow_3} = |\uparrow_1\downarrow_3\rangle\langle\uparrow_1\downarrow_3|$, $\hat{\varepsilon}_{\downarrow_1\uparrow_3} = |\downarrow_1\uparrow_3\rangle\langle\downarrow_1\uparrow_3|$ and $\hat{\varepsilon}_{\downarrow_1\downarrow_3} = |\downarrow_1\downarrow_3\rangle\langle\downarrow_1\downarrow_3|$. We find that the flips and statics are given by

$$H_{\uparrow_1\uparrow_3} = 2J\sigma_z^s + \Delta\sigma_x^s, \quad H_{\downarrow_1\downarrow_3} = -2J\sigma_z^s + \Delta\sigma_x^s, \tag{16a}$$

$$H_{\downarrow_1\uparrow_3} = H_{\uparrow_1\downarrow_3} = \Delta\sigma_x^s, \quad H_{\nu\leftarrow\mu} = \Delta\,\mathcal{I}_s, \tag{16b}$$

where ν and μ are two configurations of S' that differ by exactly *one* spin flip. The graph $\mathcal{G}$ has therefore 4 edges and is the square. The graph $\mathcal{G}$ as well as two examples for histories of S', two walks and the equivalents of Feynman diagrams are all represented in Fig. 1.

In order to make the superposition of histories manifest in the expression for $U_{\nu\leftarrow\mu}(t)$, we relabel the sum over intermediary configurations into a sum over all the walks on $\mathcal{G}$. If the initial and final configurations of S' appearing in Eq. (14) are respectively μ and ν, then the relevant walks all start on vertex v_μ and terminate on the vertex v_ν. The conditional evolution operator $U_{\nu\leftarrow\mu}$ is therefore

$$U_{\nu\leftarrow\mu}(t) = e^{-iH_\nu t}\delta_{\mu,\nu} + \sum_{n=1}^{\infty} i^{-n} \sum_{W_{\mathcal{G};\nu\mu;n}} \tag{17}$$

$$\times \int_0^t \int_0^{t_n} \dots \int_0^{t_2} e^{-iH_\nu(t-t_n)} H_{\nu\leftarrow\eta_n} e^{-iH_{\eta_n}(t_n-t_{n-1})} H_{\eta_n\leftarrow\eta_{n-1}} \dots e^{-iH_\mu t_1} dt_1 \dots dt_n,$$

where $W_{\mathcal{G};\nu\mu;n}$ is the ensemble of walks of length n on $\mathcal{G}$ from v_μ to v_ν. Eq. (17) is the central result of this work. The sum over the walks clearly identifies the successions of configurations of S' that are allowed by the Hamiltonian. Finally, Eq. (17) also presents a mathematical advantage. It points to the general approach to matrix functions from which the walk-sum method ultimately stems. This approach relies on graph-theoretic arguments with walks on graphs playing a central role [15].

2.4. Evaluation of conditional evolution operators

Conditional evolution operators are most conveniently evaluated in the the Laplace domain, because this transformation turns the nested convolutions in Eq. (17) into a product of matrices. Let $\tilde{M}_\mu(s) = \mathcal{L}\big[\exp(-iH_\mu t)\big] = (s\mathcal{I}_s + iH_\mu)^{-1}$ be the element-wise Laplace transform of $\exp(-iH_\mu t)$ with s the Laplace domain variable. It follows that the Laplace transform of a conditional evolution operator is given by

$$\tilde{U}_{\nu\leftarrow\mu}(s) = \tilde{M}_\nu(s)\delta_{\mu,\nu} + \sum_{n=1}^{\infty} \sum_{W_{\mathcal{G};\nu\mu;n}} i^{-n}\, \tilde{M}_\nu(s)\, H_{\nu\leftarrow\eta_n} \dots H_{\eta_1\leftarrow\mu}\, \tilde{M}_\mu(s). \tag{18}$$

This is the expression we use in computations. It only involves multiplications and additions of $d_s \times d_s$ matrices. Considering the case where all the $\tilde{M}_\mu(s)$ can be obtained analytically, we remark that the matrix elements of the $\tilde{M}_\mu(s)$ are ratios of polynomials in s. The roots of the denominator polynomial are $-i\lambda_\mu$ with λ_μ an eigenvalue of H_μ. This is therefore also true for any element of the sum in Eq. (18) and performing the

‡ One could equally well choose to specify the spins along another axis.

inverse transform into the time-domain can be done according to the formula

$$U_{\nu\leftarrow\mu}(t) = \sum_{\mu} \mathrm{Res}[e^{st}\tilde{U}_{\nu\leftarrow\mu}(s), -i\lambda_{\mu}], \tag{19}$$

where $\mathrm{Res}[f(s), \lambda]$ denotes the residuum of $f(s)$ at λ. In all practical situations the infinite sum in Eq. (17) is truncated at some order K. With this approximation only walks of length $n \leq K$ are taken into account. This approximation is justified because the series in Eq. (17) is absolutely and uniformly convergent for any finite time provided $\mathbb{S}$ comprises a finite number of particles. In order establish this result, we consider the contribution $U^{[K]}_{\nu\leftarrow\mu}(t)$ of all walks whose length is exactly K to $U_{\nu\leftarrow\mu}(t)$. A bound for the norm of this quantity is given by

$$\|U^{[K]}_{\nu\leftarrow\mu}(t)\| \leq a_N(K)\frac{(\Omega\, t)^K}{K!} \to 0 \quad (K \to \infty), \tag{20}$$

where $\Omega = \max_n\{\|H_{\eta_{n+1}\leftarrow\eta_n}\|\}$, $\|\cdot\|$ is the spectral norm and $a_N(K)$ is the number of walks of length K on the graph $\mathcal{G}$. In Appendix C we show that $a_N(K)$ is a polynomial in the number of particles N of the system, and hence $\|U^{[K]}_{\nu\leftarrow\mu}(t)\|$ tends to zero as $K \to \infty$. With the help of the inequality in Eq. (20) it is straightforward to show that the sequence $\mathcal{U}_K = \sum_{n=0}^{K} U^{[n]}_{\nu\leftarrow\mu}(t)$ is Cauchy, which establishes the convergence of the walk-sum series in Eq. (17). This result follows also from the convergence of the Dyson series for finite-dimensional matrices [16] and its relation to the walk-sum method (see Appendix A).

Several conclusions can be drawn from Eq. (20). First, it shows that the evaluation of walk-sum series is free from the numerical sign problem. Second, an increase in time requires to include higher order terms in Eq. (17). Third, the convergence in the evaluation of $U_{\nu\leftarrow\mu}$ can be established if an increase of the order K does not alter the result within a given accuracy. All these conclusions are confirmed by our experience with example systems in section 3 and [14].

A more detailed analysis of the convergence of walk-sum is beyond the scope of this paper. However, we emphasise that we have always observed that walk-sum converges much faster with the order K than Eq. (20) suggests. Finally, we note that conditional expectation values converge much faster than ordinary expectation values because the former quantities are insensitive to the norm of the overall state vector. In the next section we discuss how expectation values and conditional expectation values can be calculated via conditional evolution operators.

2.5. Expectation values and conditional expectation values

Here we demonstrate how conditional evolution operators can be employed for the evaluation of expectation values and conditional expectation values. For simplicity we assume that the initial state of the full system is given by $|\psi(0)\rangle = |\mu\rangle \otimes |\psi_s(0)\rangle$, where $|\psi_s(0)\rangle$ is the initial state of S§. The state vector of the full system can then be obtained via Eq. (4) and is given by

$$|\psi(t)\rangle = U(t)|\psi(0)\rangle = \sum_{\nu}\Big\{|\nu\rangle \otimes |\psi_s(t)\rangle_{\nu\leftarrow\mu}\Big\}, \tag{21}$$

§ All the relations of this sections are easily extended to more general initial pure states $\sum_{\mu} c_{\mu}|\mu\rangle \otimes |\psi_s(0)\rangle$ upon introducing a sum over μ as appropriate.

where $|\psi_s(t)\rangle_{\nu\leftarrow\mu} = U_{\nu\leftarrow\mu}(t)|\psi_s(0)\rangle$ is a piece of the wavefunction of the full system. Any mean value of an observable O can be calculated via Eq. (21). With the definition $\hat{\varepsilon}_{\nu'} O \hat{\varepsilon}_\nu = |\nu'\rangle\langle\nu| \otimes O_{\nu'\nu}$, we find

$$\langle O\rangle = \langle\psi_s(0)| \sum_{\nu',\nu} \left(U_{\nu'\leftarrow\mu}\right)^\dagger O_{\nu'\nu}\, U_{\nu\leftarrow\mu}\, |\psi_s(0)\rangle. \tag{22}$$

It follows that any expectation value of an observable O can be computed directly from conditional evolution operators if O is expanded in the projector lattice basis $\hat{\varepsilon}_\nu$.

Next we investigate in more detail the meaning of the piece $|\psi_s(t)\rangle_{\nu\leftarrow\mu} = U_{\nu\leftarrow\mu}(t)|\psi_s(0)\rangle$ of the full state vector. To this end, we write the projection of $|\psi(t)\rangle$ onto $\hat{\varepsilon}_\nu$ as

$$\hat{\varepsilon}_\nu\, |\psi(t)\rangle = |\nu\rangle \otimes |\psi_s(t)\rangle_{\nu\leftarrow\mu} = \sum_{\ell=1}^{d_s} \alpha_\ell\, |\nu\ell_s\rangle, \tag{23}$$

where the probability amplitudes α_ℓ of state $|\nu\ell_s\rangle$ (S' in configuration ν, S in state $|\ell_s\rangle$) are determined by $U_{\nu\leftarrow\mu}(t)$. This shows that $U_{\nu\leftarrow\mu}(t)$ directly evolves the projection of the full state vector $|\psi(t)\rangle$ onto a d_s dimensional subspace corresponding to S' in configuration ν. We emphasise that conditional evolution operators are submatrices of U [see Eq. (4)] and therefore not necessarily unitary. It follows that $U_{\nu\leftarrow\mu}(t)$ does generally not conserve the norm of $|\psi_s(0)\rangle$. Indeed, Eq. (23) implies that the norm of $|\psi_s(t)\rangle_{\nu\leftarrow\mu}$ is given by the probability of finding S' in configuration ν at time t, knowing that it was initially in configuration μ,

$$\langle\psi_s(0)| \left(U_{\nu\leftarrow\mu}(t)\right)^\dagger U_{\nu\leftarrow\mu}(t)\, |\psi_s(0)\rangle = \langle\hat{\varepsilon}_\nu\rangle_t. \tag{24}$$

We now turn to conditional expectation values and show that some of them can be computed directly via a single conditional evolution operator. To this end, we note that the expectation value of an arbitrary operator O_s acting on S with respect to $|\psi_s(t)\rangle_{\nu\leftarrow\mu}$ is given by

$$\langle\psi_s(0)| \left(U_{\nu\leftarrow\mu}(t)\right)^\dagger O_s\, U_{\nu\leftarrow\mu}(t)\, |\psi_s(0)\rangle = \langle O_s\hat{\varepsilon}_\nu\rangle_t, \tag{25}$$

where $\langle O_s\hat{\varepsilon}_\nu\rangle_t$ is the expectation value of $O_s\hat{\varepsilon}_\nu$ at time t. Eqs. (24, 25) directly yield the conditional expectation value $\langle O_s/\nu\rangle$ of O_s, knowing that S', initially in configuration μ, is in configuration ν at time t, ‖

$$\langle O_s/\nu\rangle = \frac{\langle O_s\hat{\varepsilon}_\nu\rangle}{\langle\hat{\varepsilon}_\nu\rangle} = \frac{\langle\psi_s(0)| \left(U_{\nu\leftarrow\mu}(t)\right)^\dagger O_s\, U_{\nu\leftarrow\mu}(t)\, |\psi_s(0)\rangle}{\langle\psi_s(0)| \left(U_{\nu\leftarrow\mu}(t)\right)^\dagger U_{\nu\leftarrow\mu}(t)|\psi_s(0)\rangle}. \tag{26}$$

Finally, Eqs. (2) and (26) imply that the full set of conditional probabilities allows one to compute the mean value of an operator acting on S, $\sum_\nu \langle O_s/\nu\rangle\langle\hat{\varepsilon}_\nu\rangle = \langle O_s\rangle$. We illustrate the preceding results in section 3, where we apply the walk-sum method to two physical systems.

3. Examples

In this section we present two examples for the walk-sum method. First we consider a simple case where 3 spins evolve according to a nearest neighbour interaction and

‖ The fact that $\langle O_s\hat{\varepsilon}_\nu\rangle/\langle\hat{\varepsilon}_\nu\rangle$ is indeed the conditional expectation value follows from $[O_s, \hat{\varepsilon}_\nu] = 0$ and $\hat{\varepsilon}_\nu^2 = \hat{\varepsilon}_\nu$ [17].

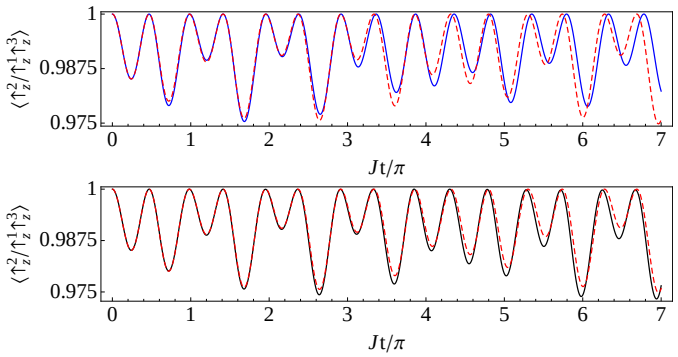

Figure 2: (Colour online). Top figure: evolution of $\langle\uparrow_2 \,/\, \uparrow_1\uparrow_3\rangle$ evaluated by walk-sum at order 2 (solid blue line) compared to the exact solution (dashed red line). Bottom figure: evolution of $\langle\uparrow_2 \,/\, \uparrow_1\uparrow_3\rangle$ evaluated by walk-sum at order 4 (solid black line) compared to the exact solution (dashed red line). Note that order 4 is the next non-zero order after order 2. Parameters: $J/\Delta = 4$.

we compare the walk-sum predictions to the exact results. Second, we consider the dynamics of a 1D chain of spin-1/2 particles interacting via strong long-range interactions.

3.1. Dynamics of 3 spins

Consider a small 1D chain with 3 spin-1/2 particles evolving according to the Hamiltonian in Eq. (15). Suppose that initially all three spins are up along z, i.e. $|\psi(0)\rangle = |\uparrow_1\uparrow_2\uparrow_3\rangle$ and suppose that we are interested in the time evolution of the conditional expectation value $\langle\uparrow_2 \,/\, \uparrow_1\uparrow_3\rangle$. This is the probability for spin 2 to be up along z knowing the other 2 spins are up along z. To implement walk-sum, we take S to be the spin 2 and S' comprises spins 1 and 3. Similarly to the example of section 2.3, we choose the configurations of S' to specify the direction of these spins along the z-axis and obtain the flips and statics of Eq. (16). The graph $\mathcal{G}$ is the square represented in Fig. 1. According to Eq. (26), the quantity $\langle\uparrow_2 \,/\, \uparrow_1\uparrow_3\rangle$ is given by

$$\langle\uparrow_2 \,/\, \uparrow_1\uparrow_3\rangle = \frac{\langle\psi_s(0)|\big(U_{\uparrow_1\uparrow_3\leftarrow\uparrow_1\uparrow_3}\big)^\dagger P_{\uparrow_2} U_{\uparrow_1\uparrow_3\leftarrow\uparrow_1\uparrow_3}|\psi_s(0)\rangle}{\langle\psi_s(0)|\big(U_{\uparrow_1\uparrow_3\leftarrow\uparrow_1\uparrow_3}\big)^\dagger U_{\uparrow_1\uparrow_3\leftarrow\uparrow_1\uparrow_3}|\psi_s(0)\rangle}, \tag{27}$$

where $P_{\uparrow_2} = |\uparrow_2\rangle\langle\uparrow_2|$ and $|\psi_s(0)\rangle = |\uparrow_2\rangle$ is the initial state of subsystem S. Considering the closed walks off vertex $v_{\uparrow_1\uparrow_3}$ on $\mathcal{G}$ and keeping only walks of length 2 or less, the conditional evolution operator in the Laplace domain $\tilde{U}_{\uparrow_1\uparrow_3\leftarrow\uparrow_1\uparrow_3}$ is given by

$$\tilde{U}_{\uparrow_2\uparrow_3\leftarrow\uparrow_2\uparrow_3}(s) \simeq \overbrace{\tilde{M}_{\uparrow_1\uparrow_3}}^{\text{Walk of length 0}} + (-i\Delta)^2 \overbrace{\tilde{M}_{\uparrow_1\uparrow_3}(\tilde{M}_{\downarrow_1\uparrow_3} + \tilde{M}_{\uparrow_1\downarrow_3})\tilde{M}_{\uparrow_1\uparrow_3}}^{\text{Two walks of length 2}}, \tag{28}$$

where the factor $(-i\Delta)^2$ comes from the flips. The two walks of length two taken into account here are those highlighted by solid-red and dashed-blue lines in Fig. 1. In Fig. 2 we compare the walk-sum result for the time evolution of $\langle\uparrow_2 \,/\, \uparrow_1\uparrow_3\rangle$ to the exact result. For short times $Jt \lesssim 3\pi$, the agreement between the walk-sum estimation of

$\langle\uparrow_2 / \uparrow_1\uparrow_3\rangle$ at order 2 and the exact result is excellent. Differences appear for $Jt \gtrsim 3\pi$ and grow larger with time. At order 4, which is the next non-zero order, the difference between the walk-sum estimation and the exact result does not exceed 5×10^{-3} for t up to $Jt \sim 7\pi$, which represents a relative error of less than 0.5%.

3.2. Dynamics of a 1D spin chain with long-range interactions

In our second example we demonstrate that the walk-sum method allows one to investigate the quantum dynamics of systems with long-range interactions. More specifically, we consider a one-dimensional chain comprised of 27 spin-1/2 particles that is described by the Hamiltonian

$$H = \sum_i \Big\{ \Delta P^i - \frac{1}{2}\Omega\, \sigma_x^i + \frac{1}{2} \sum_{j\neq i} \frac{U}{|i-j|^3} P^i P^j \Big\}, \tag{29}$$

where Δ, Ω and U are real parameters and we introduced the Pauli matrix σ_x^i of spin i. Throughout this section, we choose the z axis as the quantisation axis and take the eigenstates $|\uparrow_i\rangle$ and $|\downarrow_i\rangle$ of the Pauli matrix σ_z^i as basis states of spin i. Furthermore, we set $P^i = |\uparrow_i\rangle\langle\uparrow_i| = (\mathcal{I} + \sigma_z^i)/2$ and $G^i = |\downarrow_i\rangle\langle\downarrow_i| = (\mathcal{I} - \sigma_z^i)/2$. The term proportional to U in Eq. (29) describes a long-range interaction between the spins that scales as $1/R^3$ with the distance R between two spins.

We now study the real-time dynamics of the conditional expectation value $\langle\uparrow_c/\uparrow_j\rangle = \langle\uparrow_c\uparrow_j\rangle/\langle\uparrow_j\rangle$, where $\langle\uparrow_c\uparrow_j\rangle$ ($\langle\uparrow_j\rangle$) is the probability for spins c and j (spin j) pointing upwards. $\langle\uparrow_c/\uparrow_j\rangle$ describes the probability that spin c at the centre of the lattice is in state $|\uparrow_c\rangle$, knowing that spin $j \neq c$ is pointing upwards as well. For the implementation of walk-sum, we choose $S \equiv c$ to be the spin at the centre of the lattice and assume that all spins are initially prepared in $|\downarrow\rangle$. We choose the projector-lattices to be tensor products of projectors P^i and G^i on S',

$$\hat{\varepsilon}_{i_1\ldots i_n} = \otimes_{r\in S'\setminus\{i_1\ldots i_n\}} G^r \ \otimes_{i_\ell\in\{i_1\ldots i_n\}} P^{i_\ell} \otimes \mathcal{I}_s. \tag{30}$$

The projector lattice $\hat{\varepsilon}_{i_1\ldots i_n}$ projects S' in a state where all spins at positions $i_1 \ldots i_n$ are pointing upwards, and all other spins of S' are pointing downwards. With this definition, we find that the flips are given by

$$H_{i_1\ldots i_{n\pm1}\leftarrow i_1\ldots i_n} = -\frac{1}{2}\,\Omega\,\mathcal{I}_s, \text{ and 0 otherwise,} \tag{31}$$

that is $H_{\nu\leftarrow\mu} \neq 0$ if and only if ν differs from μ by exactly one spin flip. The evaluation of the statics yields t

$$H_{i_1\ldots i_n} = \Big(n\Delta + \frac{1}{2} \sum_{\substack{i_p\neq i_\ell \\ (i_p,i_\ell)\in\{i_1\ldots i_n\}}} \frac{U}{|i_p - i_\ell|^3}\Big)\mathcal{I}_s + \Big(\Delta + \sum_{i_p\in\{i_1\ldots i_n\}} \frac{U}{|s-i_p|^3}\Big)P^s - \frac{1}{2}\Omega\,\sigma_x^s. \tag{32}$$

The conditional expectation value $\langle\uparrow_c / \uparrow_j\rangle = \langle\uparrow_c\uparrow_j\rangle/\langle\uparrow_j\rangle$ is composed of the probabilities $\langle\uparrow_c\uparrow_j\rangle$ and $\langle\uparrow_j\rangle$. These quantities can be computed via Eq. (22),

$$\langle\uparrow_s\uparrow_j\rangle = \langle\downarrow_s| \sum_{\eta(j)} \big(U_{\eta(j)\leftarrow\downarrow_s}\big)^\dagger P^s\, U_{\eta(j)\leftarrow\downarrow_s} |\downarrow_s\rangle, \tag{33a}$$

$$\langle\uparrow_j\rangle \quad = \langle\downarrow_s| \sum_{\eta(j)} \big(U_{\eta(j)\leftarrow\downarrow_s}\big)^\dagger U_{\eta(j)\leftarrow\downarrow_s} |\downarrow_s\rangle. \tag{33b}$$

In this equation, the sum runs over all configurations $\eta(j)$ of S' where spin j is pointing upwards. We compute the conditional evolution operators $U_{\eta(j)\leftarrow\downarrow_s}$ in the Laplace

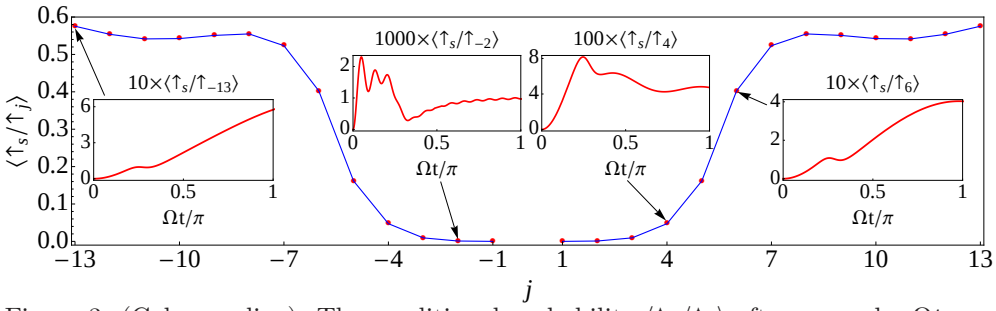

Figure 3: (Colour online). The conditional probability $\langle\uparrow_s/\uparrow_j\rangle$ after a π-pulse $\Omega t = \pi$ with $\Delta = 0$ and $U = -200\Omega$. Subsystem S is represented by the central spin (label 0). Insets show the time evolution of $\langle\uparrow_s/\uparrow_j\rangle$ for $j = -13,\ -2,\ 4$ and 6.

domain via Eq. (18). For example, the conditional evolution operator $\tilde{U}_{j\leftarrow 0}$ with only spin j pointing upwards in the final configuration $\eta(j)$ of S' and for walks of length $n \leq 3$ is given by

$$\tilde{U}_{j\leftarrow 0}(s) \simeq \frac{i\Omega}{2}\tilde{M}_j\tilde{M}_0 + \left(\frac{i\Omega}{2}\right)^3 \sum_{\substack{p=1 \\ p\neq j,\ p\neq s}}^{27} \tilde{M}_j(\tilde{M}_0 + \tilde{M}_{j,p})(\tilde{M}_p + \tilde{M}_j)\tilde{M}_0. \qquad (34)$$

In this expression, the factors $i\Omega/2$ and $(i\Omega/2)^3$ come from the flips and $\tilde{M}_{i_1\ldots i_n}(s) = \mathcal{L}\big[\exp(-iH_{i_1\ldots i_n}t)\big]$, where the static $H_{i_1\ldots i_n}$ is defined in Eq. (32). The sum over p in Eq. (34) accounts for an up-spin in an intermediary configuration of S' that is not present in the initial and final configurations. Note that intermediary spin-excitations are similar to virtual particles appearing in the Feynman diagrams of QED. This observation further substantiates the analogy between the walk-sum method and path-integrals.

In the evaluation of Eq. (33) we consider all configurations $\eta(j)$ of S' with at most 4 up-spins. For each conditional evolution operator we took into account all walks of length 4 or shorter, i,e., we truncated the series in Eq. (18) at $n = 4$. We find that these approximations are justified because the result for $\langle\uparrow_s/\uparrow_j\rangle$ converges with the terms taken into account and for the chosen parameters. In particular, we consider the regime $U \gg \Omega$ where the interaction U between nearby spins dominates the coherent driving term $\Omega\,\sigma_x^j/2$ in Eq. (29). In this case, the strong interaction inhibits the simultaneous excitation of two nearby spins, and only configurations of S' with a few, evenly distributed up-spins will contribute significantly to Eq. (33).

The final result for $\langle\uparrow_s/\uparrow_j\rangle$ in the time domain is shown in Fig. (3). Note that $\langle\uparrow_s/\uparrow_j\rangle$ is much smaller than unity for $|j| \lesssim 6$. It follows that the excitation probability for the central spin at site 0 (subsystem S) is very small if another spin at site $|j| \leq 6$ is pointing upwards. This result is characteristic of a blockade effect [18, 19, 20] that is well known for Rydberg atoms coupled by the dipole-dipole interaction. Indeed, we show in Appendix B that a physical realization of the Hamiltonian in Eq. (29) can be achieved with a one-dimensional chain of atoms in their ground states that are subsequently laser-excited to Rydberg states.

4. Computational cost: polynomial scaling in N

In this section we show that the number of floating point operations required to approximate a conditional evolution operator to order K scales polynomially in the

number of particles N of the system. For simplicity and without loss of generality, we assume that all particles have d internal levels and that S contains p particles, and thus $d_s = d^p$. The evaluation of a single walk of length K to a conditional evolution operator requires $2K + 1$ multiplications of $d_s \times d_s$ matrices (K statics and $K + 1$ flips), i.e. $\sim 2Kd_s^3$ operations. Then all the walk contributions must be added together. This represents an additional $|W_{\mathcal{G};\nu\mu;K}|d_s^2$ operations, $|W_{\mathcal{G};\nu\mu;K}|$ being the number of walks of length K on $\mathcal{G}$ between vertices v_ν and v_μ. We show in Appendix C that $|W_{\mathcal{G};\nu\mu;K}| < \text{poly}(N)$ is always bounded by a *polynomial* in N. This is a direct consequence of the sparsity of quantum Hamiltonians: there are not so many configurations accessible to S' through K jumps. An upper bound for the number of operations $\mathcal{N}_K$ required to obtain $U_{\mu\leftarrow\nu}$ at order K is therefore given by

$$\mathcal{N}_K < (2Kd_s^3 + d_s^2)\,\text{poly}(N). \tag{35}$$

It follows that the computational cost for the evaluation up to order K of a single conditional evolution operator scales polynomially with the number of particles N. On the contrary, the progression of the accuracy with the order K and the number of particles N are open questions. However, we find that the accuracy of walk-sum at a given order K exhibits a very weak dependence on N in the case of the example in section 3.2. This observation suggests that the walk-sum method scales polynomially in the number of particles N for strongly interacting spin chains where blockade effects limit the total number of excitations in the lattice.

5. Conclusion

We have introduced the walk-sum that allows one to investigate the real-time dynamics of quantum systems. We have shown that walk-sum can approximate any desired piece of an evolution operator independently of any other. Furthermore, the number of operations involved in approximating any such piece at order K scales polynomially with the system size. This result holds independently of the system geometry and the nature of its interactions. We find that the walk-sum method is very well suited for the study of strongly interacting spin chains where blockade effects limit the number of final excitations in the lattice. Note that a physical realisation of these systems is given by Rydberg atoms interacting via the long-range dipole-dipole interaction. These systems are well confined to a part of their state space whose size grows polynomially with the number of particles. In addition to the efficient approximation of single conditional evolution operators, these systems allow one to approximate the *entire* evolution operator with moderate computational effort. The reason is that the number of all conditional evolution operators contributing substantially to the norm of the state vector scales polynomially with the number of particles N.

Walk-sum is similar to Feynman path-integrals in that it describes a quantum evolution as resulting from the superposition of all the possible histories of the system. It differs from path-integrals in that it is well adapted to systems with discrete degrees of freedom and can independently evolve any chosen sub-ensemble S of an otherwise large many-body system. We will show elsewhere that walk-sum can be extended to systems with continuous degrees of freedom. In this case, and if S has only one internal level, then the walk-sum method is formally equivalent to path-integrals.

Walk-sum is also well suited to describe the effect of post-selection in quantum systems. Indeed, since a conditional evolution operator specifies both the initial and

final configurations of S', walk-sum is really a time-symmetric description of quantum mechanics. In particular, we will show that the Aharonov-Bergmann-Lebowitz rule of the Two State Vector Formalism [21] follows from a simple constraint on the walks of the graph $\mathcal{G}$ and is straightforwardly demonstrated with conditional evolution operators.

Finally, it is worth noting that the deep origin of the computational speed-up achieved by walk-sum resides in exact summations of infinite families of terms performed at the graph-theoretic level by Eq. (17, 18). These resummations make walk-sum fundamentally different from power series and are explicitly apparent in the full graph theoretic treatment provided in [15]. In fact, further resummations are possible that reduce the sum over walks into a sum over simple paths, a simple path being forbidden to visit any vertex more than once. The resulting method, called path-sum is nonperturbative and computes any conditional evolution operator *exactly* in a *finite* number of operations. Path-sum can be also seen as a generalisation of the method of resolvents. Its use for the study of quantum dynamics will be exposed elsewhere.

Acknowledgments

P-L Giscard is supported by Scatcherd European and EPSRC scholarships. M Kiffner thanks Wenhui Li and Tom F Gallagher for discussions.

Appendix A. Alternative derivation of Eq. (12)

Here we provide an alternative derivation of Eq. (12) for $\hat{\varepsilon}_\nu U(t)\hat{\varepsilon}_\mu$ via the well-known expression (see, e.g., Complement AI.2 in [22])

$$U(t,0) = \exp[-i(H_0+V)t] = \exp[-iH_0 t] + \sum_{n=1}^{\infty} \times i^{-n} \int_0^t \int_0^{t_n} \cdots \int_0^{t_2} e^{-iH_0(t-t_n)} V e^{-iH_0(t_n-t_{n-1})} V \ldots e^{-iH_0 t_1} dt_1 \ldots dt_n, \tag{A.1}$$

which is used in time-dependent perturbation theory. In order to establish Eq. (12) via Eq. (A.1), we expand the Hamiltonian H in terms of the complete set of projector-lattices in Eq. (2) and obtain $H = H_0 + V$, where

$$H_0 = \sum_\nu \hat{\varepsilon}_\nu H \hat{\varepsilon}_\nu, \quad V = \sum_{\nu \neq \mu} \hat{\varepsilon}_\nu H \hat{\varepsilon}_\mu. \tag{A.2}$$

If these expressions are plugged in Eq. (A.1), the orthogonality of the projector lattices directly yields the result in Eq. (12). This indicates another interpretation for the result of Eq. (12): the transitions undergone by S' can be seen as perturbations affecting the evolution of S.

Appendix B. Rydberg-excited Mott insulators

In this section we discuss a physical realization of the Hamiltonian in Eq. (29). We consider a one-dimensional chain of atoms that are prepared in the Mott-insulating phase with unit filling via a strong optical lattice. An external laser field couples the ground state $|g\rangle$ of each atom to a Rydberg state $|r\rangle$. We assume that atomic transitions to other internal levels are negligible such that the atoms are well described

by two-level systems. Two Rydberg atoms at lattice site i and j interact via the long-range dipole-dipole interaction that is of the form [23]

$$A_{ij} = (4\pi\epsilon_0 R_{ij}^3)^{-1}\big[\boldsymbol{\mu_i}.\boldsymbol{\mu_j} - 3R_{ij}^{-2}(\boldsymbol{\mu_i}.\boldsymbol{R_{ij}})(\boldsymbol{\mu_j}.\boldsymbol{R_{ij}})\big], \tag{B.1}$$

where $\boldsymbol{R_{ij}}$ is the relative distance between atoms i and j, and $\boldsymbol{\mu_i}$ is the dipole moment of atom i. We assume that all dipole moments are identical and oriented along the axis of the lattice. With $\mu = \mu_i = \|\boldsymbol{\mu}_i\|$, the dipole-dipole interaction can be written as $A_{ij} = -2\mu^2(4\pi\epsilon_0 L^3)^{-1}/|i-j|^3$, where L is the lattice constant. It follows that the chain of laser-driven atoms is described by the Hamiltonian in Eq. (29) if we set $U = -2\mu^2(4\pi\epsilon_0 L^3)^{-1}$ and if we employ the frozen gas and rotating-wave approximations. In this case, Δ describes the laser detuning with the $|g\rangle \leftrightarrow |r\rangle$ transition, Ω is the Rabi frequency of the driving laser field, and the spin states $|\uparrow\rangle$ and $|\downarrow\rangle$ correspond to $|r\rangle$ and $|g\rangle$, respectively. The quantity $\langle\uparrow_s/\uparrow_j\rangle$ describes the probability for atom s being in its Rydberg state $|r_s\rangle$ knowing that atom j is excited as well. In particular, Fig. (3) corresponds to the following physical parameters: time $\Omega t = \pi$, lattice spacing $L = 4\mu$m, laser detuning $\Delta = 0$, Rabi frequency $\Omega = 5$MHz and dipole moment $\mu \simeq 2350 e a_0$ (Rydberg level principal number ≈ 40).

Appendix C. An upper bound for the number of walks

Here we derive an upper bound for $|W_{\mathcal{G};\nu\mu;n}|$ the number of walks of length n between two vertices v_μ and v_ν on a graph $\mathcal{G}$. We employ the same notation and definitions as in section 4. Suppose that the flips of the Hamiltonian H of $\mathbb{S}$ [see Eq. (13)] are only non-zero for those configurations μ and ν of S' where at most q particles change their state in a transition from μ to ν. For example, the expressions for the flips in Eqs. (16) and (31) demonstrate that the Hamiltonians in Eqs. (15) and (29) have $q = 1$. In fact, most of the common Hamiltonians have $q = 1,\ 2$. With p particles in S there are $N-p$ particles in S', and thus there are $\binom{N-p}{q}$ ways to choose which q particles among $N-p$ undergo a transition. Furthermore, for each particle that changes a state there are at most $d-1$ possible basis states available for the transition. In total, there are thus at most $V < \binom{N-p}{q}(d-1)^q$ configurations directly accessible to S' from any given one. By construction of $\mathcal{G}$, this is also an upper-bound on the number of vertices that share an edge with any given vertex on $\mathcal{G}$. It follows that there are at most V^n walks of length n attached to any vertex of $\mathcal{G}$, and thus we find

$$|W_{\mathcal{G};\nu\mu;n}| < \tbinom{N-p}{q}^n (d-1)^{qn}, \tag{C.1}$$

which scales polynomially in $N-p$ for small q. Note that this upper-bound is very loose and we only use it to demonstrate that $|W_{\mathcal{G};\nu\mu;n}|$ is always bounded by a polynomial in N. For example, for a system with $N+1$ spin-1/2 particles, one particle in S ($p = 1$) and a Hamiltonian with $q = 1$, the graph $\mathcal{G}$ is the N-hypercube. In this case, we find that the number of walks of length $n = \ell + 2k > 0$, $k \in \mathbb{N}$, $0 \le \ell \le N$, between two vertices separated by a distance ℓ is

$$a_N(\ell+2k) = \frac{2}{2^N}\sum_{i=0}^{\lfloor N/2\rfloor}(2i+p_N)^{\ell+2k}\sum_{j=0}^{\lfloor N/2\rfloor}\binom{N-\ell}{\lfloor\frac{N}{2}\rfloor - i - j}\binom{\ell}{j}(-1)^j, \tag{C.2}$$

where $p_N = N \bmod 2$ and $\lfloor\cdot\rfloor$ is the floor function. This is substantially smaller than the $N^{\ell+2k}$ of the bound Eq. (C.1), indeed for $N \gg 1$, $N \gg n$, $a_N(\ell+2k) \sim 2^{-k}(N - \ell/2 - 1)^k(\ell+2k)!/k! \ll N^{\ell+2k}$ and for $n \gg N$, $a_N(\ell+2k) \sim 2^{-N+1}\,N^{\ell+2k} \ll N^{\ell+2k}$.

References

[1] W. S. Bakr , J. I. Gillen, A. Peng, S. Fölling, and M. Greiner. A quantum gas microscope for detecting single atoms in a hubbard-regime optical lattice. *Nature*, 462:74, 2009.

[2] J. F. Sherson, C. Weitenberg, M. Endres, M. Cheneau, I. Bloch, and S. Kuhr. Single-atom-resolved fluorescence imaging of an atomic mott insulator. *Nature*, 467:68, 2010.

[3] W. S. Bakr, A. Peng, M. E. Tai, R. Ma, J. Simon, J. I. Gillen, S. Fölling, L. Pollet, and M. Greiner. Probing the superfluid-to-mott insulator transition at the single-atom level. *Science*, 329:547, 2010.

[4] C. Weitenberg, M. Endres, J. F. Sherson, M. Cheneau, P. Schauß, T. Fukuhara, I. Bloch, and S. Kuhr. Single-spin addressing in an atomic mott insulator. *Nature*, 471:319, 2011.

[5] M. Lewenstein, A. Sanpera, V. Ahufinger, B. Damski, A. Sen De, and U. Sen. Ultracold atomic gases in optical lattices: mimicking condensed matter physics and beyond. *Adv. Phys.*, 56:243, 2007.

[6] S. R. White. Density matrix formulation for quantum renormalization group. *Phys. Rev. Lett.*, 69:2863, 1992.

[7] J. I. Cirac and F. Verstraete. Renormalization and tensor product states in spin chains and lattices. *J. Phys. A: Math. Theor.*, 42:504004, 2009.

[8] G. Vidal. Efficient classical simulation of slightly entangled quantum computations. *Phys. Rev. Lett.*, 91:147902, 2003.

[9] F. Verstraete, V. Murg, and J. I. Cirac. Matrix product states, projected entangled pair states, and variational renormalization group methods for quantum spin systems. *Adv. Theor. Phys.*, 57:143, 2008.

[10] E. Jeckelman. Density-matrix renormalization group methods for momentum- and frequency-resolved dynamical correlation functions. *Prog. Theor. Phys. Suppl.*, 176:143, 2008.

[11] N. Shibata. Quantum hall systems studied by the density matrix renormalization group method. *Prog. Theor. Phys. Suppl.*, 176:182, 2008.

[12] F. Verstraete and J. I. Cirac. Renormalization algorithms for quantum-many body systems in two and higher dimensions. *arXiv:cond-mat/0407066v1*, 2004.

[13] Z.-C. Gu and X.-G. Wen. Tensor-entanglement-filtering renormalization approach and symmetry-protected topological order. *Phys. Rev. B*, 80:155131, 2009.

[14] P.-L. Giscard and D. Jaksch. Transient crystals and tunable supersolids of rydberg excitations. *arXiv:1108.1177 [quant-ph]*, 2011.

[15] P.-L. Giscard, S. Thwaite, and D. Jaksch. Evaluating matrix functions by resummations on graphs: the method of path-sums. *arXiv:1112.1588v1 [math.QA]*, 2011.

[16] E. Zeidler. *Quantum Field Theory I: Basics in Mathematics and Physics. A Bridge between Mathematicians and Physicists*. Springer, 2006.

[17] G. Niestegge. An approach to quantum mechanics via conditional probabilities. *Found. Phys.*, 38:241, 2008.

[18] R. Heidemann *et al.* Evidence for coherent collective rydberg excitation in the strong blockade regime. *Phys. Rev. Lett.*, 99:163601, 2007.

[19] A. Gaëtan, Y. Miroshnychenko, T. Wilk, A. Chotia, M. Viteau, D. Comparat, P. Pillet, A. Browaeys, and P. Grangier. Observation of collective excitation of two individual atoms in the rydberg blockade regime. *Nature Phys.*, 5:115, 2009.

[20] T. Pohl, E. Demler, and M. D. Lukin. Dynamical crystallization in the dipole blockade of ultracold atoms. *Phys. Rev. Lett.*, 104:043002, 2010.

[21] Y. Aharonov and L. Vaidman. Complete description of a quantum system at a given time. *J. Phys A: Math. Gen.*, 24:2315, 1991.

[22] C. Cohen-Tannoudji, J. Dupont-Roc, and G. Grynberg. *Atom-Photon Interactions*. J. Wiley & Sons, 1998.

[23] D. Jaksch, J. I. Cirac, P. Zoller, S. L. Rolston, R. Côté, and M. D. Lukin. Fast quantum gates for neutral atoms. *Phys. Rev. Lett.*, 85:2208, 2000.